Physics of the Solid State, 2024, Vol. 66, No. 10

06,07

Influence of the modification methods on the crystal structure and macroresponses of the multicomponent ferroelectric media based on sodium-potassium niobates

© L.A. Shilkina[1], E.V. Glazunova[1], S.I. Dudkina[1], D.V. Volkov[2], L.A. Reznichenko[1]

[1] Scientific Research Institute of Physics, Southern Federal University,
Rostov-on-Don, Russia
[2] Institute of High Technologies and Piezotechnics of the Southern Federal University,
Rostov-on-Don, Russia
E-mail: lid-shilkina@yandex.ru

Received August 19, 2024
Revised August 26, 2024
Accepted August 27, 2024

The superstoichiometrical and stoichiometrical modification of the solid solutions (SS) of the multi-element system $0.98(Na_{0.54}K_{0.46})(Nb_{0.9}Ta_{0.1})O_3-0.02LiSbO_3$ by plain (MnO_2, CuO) and combined (MnO_2+NiO, $Bi_2O_3+Fe_2O_3$) oxides was studied. The samples were obtained by two-stage solid-phase synthesis followed by sintering using conventional ceramic technology. Based on the analysis of X-ray studies, it was established that the initial solid solution has an orthorhombic symmetry with a monoclinic perovskite cell R(M). The modification of it, both stoichiometrical and superstoichiometrical, with the specified modifiers, leads to the appearance of a second, tetragonal phase inside the orthorhombic R(M) phase, i. e., transfers the solid solution to the morphotropic phase transition region. With both modification schemes, the density of the modified ceramics increases compared to the density of the original solid solution; at the same time in the superstoichiometrically modified solid solutions, the stability of the structure to small fluctuations in composition was revealed. The compositions with superstoichiometrical modification by MnO_2 and $Bi_2O_3+Fe_2O_3$ oxides have high-quality piezoelectric parameters and can be recommended for applications in microwave technology.

Keywords: alkali metal niobates, phase, alloying.

DOI: 10.61011/PSS.2024.10.59633.217

1. Introduction

A binary system based on sodium-potassium niobates ((Na,K)NbO_3, NKN) is one of the most studied lead-free ferroactive systems, which is not inferior, and may have been recently superior in popularity to the lead zirconate-titanate system ($Pb(Zr,Ti)O_3$, PZT) which is the basis of the vast majority of industrially produced piezotechnical materials. The interest in the NKN system is driven primarily by its environmental safety (unlike PZT media containing extremely toxic lead), as well as the similarity of the main electrophysical characteristics of solid solutions (SS) of both systems from the morphotropic phase transition region (morphotropic region, MR) with equal quantities of extreme components (Table 1).

In addition, the wide isomorphism of the niobate system, as well as PZT-system, with the relative simplicity of the perovskite structure, makes it possible to modify it by small variations in the cationic composition, as well as the molecular design based on the construction of multicomponent media. The introduction of new compounds forming solid solutions with the components of the initial system allows changing the composition in a wide range, and therefore the parameters of solid solution, and obtaining a wide variety of material properties. As a result, materials for various applications can be on the basis of a single multicomponent system, which is convenient for their production. The dimensionality of the MR, as well as the dimensionality of adjacent areas of the phase diagram, increases with an increase of the number of components, which significantly expands the possibilities of choosing a solid solution with a given combination of characteristics. As noted in Ref. [2], multicomponence, as a rule, (with a certain number of components) contributes to improving the manufacturability of systems. This is attributable to the fact that heterovalent substitutions result in the formation of an additional concentration of point defects with an increase of the set of ions in the solid solution and these point defects contribute to the intensification of diffusion phenomena, mass transfer and, as a result, synthesis processes, sintering, formation of optimal microstructure and macro-reactions of materials.

A large group of similar NKN-based systems consists of compositions with Li-containing compounds of various compositions ($LiNbO_3$, $LiSbO_3$, $LiTaO_3$) to name a few, ensuring a sufficiently high level of piezoactivity of the basic niobate system [3–18].

We also determined the impact of thermodynamic prehistory on the possibility of obtaining high-density pure ferroelectric ceramics in a se-

Table 1. Electrophysical characteristics of solid solutions of NKN and PZT-systems from the morphotropic region (according to [1])

Material	$\varepsilon_{33}^{T}/\varepsilon_0$	$\lvert d_{31}\rvert$, pC/N	d_{33}, pC/N	$\lvert g_{31}\rvert$, mV · m/N	g_{33}, mV · m/N	K_p	Q_M	T_C, °C
NKN	290* (420)**	32 (49)	80 (160)	12.6 (13.1)	31.5 (43)	0.36 (0.45)	130 (240)	390 (400)
PZT	730	93.5	223	14.5	34.5	0.52	500	386

Note. Materials fabrication method: * by conventional ceramic processing (CCP); ** by hot pressing (HP) (data in parentheses).

ries of articles [19–23] dedicated to the system of solid solutions $[(Na_{0.5}K_{0.5})_{1-x}Li_x](Nb_{1-y-z}Ta_ySb_z)O_3$ with $x = 0.00-0.14$, $y = 0.01$; 0.20; $z = 0.00-0.10$, $\Delta z = 0.01$, evaluated the dynamics of behavior of materials under the field in the process of polarization, studied the deformation, polarization and reversible characteristics of solid solutions, including solid solutions modified by simple and combined additives.

This paper examines the effect of the method of modification (stoichiometric, superstoichiometric) on the crystal structure and macro-responses of selected samples continuing and developing previously conducted studies.

2. Objects, methods for obtaining and studying of samples

The objects of the study were solid solutions based on a multi-element composition of $0.98(Na_{0.54}K_{0.46})(Nb_{0.9}Ta_{0.1})O_3-0.02LiSbO_3$, including solid solutions modified by simple (MnO_2, CuO) and combined $(MnO_2+NiO$, $Bi_2O_3+Fe_2O_3)$ oxides, that were superstoichiometrically inserted in quantities of 1−3 mass.% and stoichiometrically inserted in quantities of $x = 0.0125-0.0375$. The samples were synthesized by a two-stage method of solid-phase reactions at $T_{\text{syn1}} = 880°C$, $t_{\text{syn1}} = 6\,h$; $T_{\text{syn2}} = 900°C$, $\tau_{\text{syn2}} = 4\,h$; sintering was performed using conventional ceramic processing at $T_{\sin} = 1155-1200°C$ and $\tau_{\sin} = 1.0-1.5\,h$ depending on the composition. Optimal procedures for the process of obtaining objects were established using a series of samples with X-ray and microstructural control, taking into account the values of the measured sample densities.

Sintered ceramic workpieces in the form of discs with a diameter of 12 mm and a thickness of 3 mm were machined (grinding on flat surfaces and ends) to obtain measuring samples with a diameter of 10 × 1 mm, which were further calcined at 500°C for 0.5 h for removal of organic substance residues and for degreasing surfaces improving the adhesion of the metal coating (electrodes) with ceramics. The latter were applied by double burning of a silver-containing paste at 800°C for 0.5 h.

The samples were polarized in a polyethylene siloxane liquid at a temperature of 120−140°C and with an electric field strength of 4.0−7.0 kV/mm for 0.25 h, followed by cooling under the field to room temperature for 0.5 h. Additional exposure under the field at room temperature and preheating of ceramics without the application of a field were used for minimizing the negative effects of hydrolysis products, which are often formed during the synthesis of media based on alkali metal niobates. X-ray studies were performed by the powder diffraction method using DRON-3 diffractometer with CoKα radiation (Bragg-Brentano focusing arrangement). Powdered ceramics were studied to eliminate stresses and textures that occur during the fabrication of ceramics. The cell parameters were calculated using quadratic shapes corresponding to the symmetry of the crystal lattice [24]. The errors of measurement of structural parameters have the following values: linear — $\Delta a = \Delta b = \Delta c = \pm(0.002-0.004)$ Å, angular — $\Delta\beta = \pm 0.05°$, volume — $\Delta V = \pm(0.05-0.1)$ Å^3.

The measured (experimental) density of the samples, ρ_{exp}, was determined by hydrostatic weighing in octane. The X-ray density was calculated using the formula $\rho_{\text{X-ray}} = MZ/(N_A V)$, where M —molecular weight, Z — number of formula units per lattice cell, N_A — Avogadro number, and V — lattice cell volume, $\rho_{\text{rel}} = \rho_{\text{exp}}/\rho_{\text{X-ray}} \cdot 100\%$.

The electrophysical properties of objects at a room temperature were characterized by determining of the relative dielectric permittivity of nonpolarized, $\varepsilon/\varepsilon_0$, ($\varepsilon_0$ — the dielectric constant of vacuum, equal to $8.85 \cdot 10^{-12}$ F/m) and polarized, $\varepsilon_{33}^{T}/\varepsilon_0$, samples in accordance with Ref. [25]; piezomodules d_{ij}, electromechanical coupling coefficients K_{ij}, mechanical Q-factor Q_M, sound velocity V_1^E, Curie temperatures T_C. Measurement errors — $\varepsilon_{33}^{T}/\varepsilon_0 \le \pm 1.5\%$, $K_p \le \pm 2\%$ (K_p — electromechanical coupling coefficient of the radial oscillation mode), $\lvert d_{31}\rvert \le \pm 4\%$, $Q_M \le \pm 12\%$.

3. Experimental results and discussion

It was found by X-ray studies that the initial solid solution has rhombic symmetry with a monoclinic perovskite cell R(M), the parameters of which are $a = c = 3.995$ Å, $b = 3.945$ Å, $\beta = 90.21°$, $V = 62.97$ Å^3. The X-ray pattern of the initial solid solution and the diffraction peaks $(200)_C$ and $(220)_C$ are shown in Figure 1 in an enlarged scale. The apparent splitting of the diffraction peaks 200 and 220 indicates that the solid solution is heterogeneous and actually consists of several low-symmetry phases with similar cell parameters. The effect is quite expected, since the difference in the ionic radii of A-cations, attributed to a

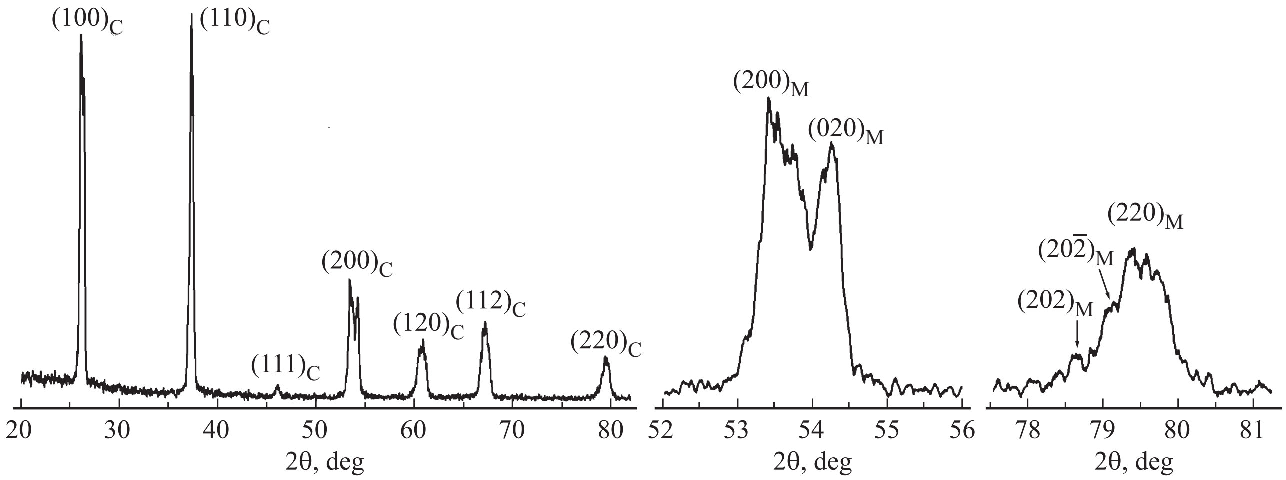

Figure 1. X-ray pattern of the initial TR and diffraction peaks $(200)_C$ and $(220)_C$ at an enlarged scale.

Table 2. Ionic radii R and electronegativities EN of the cations in the composition of the initial solid solution and modifiers

Cations		R, Å at CN 6 [27]	EN [28]
A	Na^{1+}	0.98	0.9
	K^{1+}	1.33	0.8
	Li^{1+}	0.78	1.0
B	Nb^{5+}	0.66	1.6
	Sb^{5+}	0.62	1.9
	Ta^{5+}	0.66	1.5
Modifiers	Bi^{3+}	1.20	1.9
	Cu^{2+}	0.80	1.9
	Fe^{3+}	0.67	1.8
	Mn^{4+}	0.52	1.5
	Ni^{2+}	0.74	1.9

smaller value, far exceeds the permissible value of 15% [26]. For example, ΔR (K-Na) — 36%, and ΔR (K-Li) — 70% (see Table 2).

Given the complex formula composition of the studied solid solutions, it can be expected that they may contain an R(M) phase with a large angle β corresponding to $Na_{1-x}Li_xNbO_3$ solid solution with a low Li content in addition to the main R(M)-phase with a small angle β, characteristic of $Na_{0.54}K_{0.46}NbO_3$ solid solution.

Let us consider the effects of modification of $0.98(Na_{0.54}K_{0.46})(Nb_{0.9}Ta_{0.1})O_3{-}0.02LiSbO_3$ solid solution by manganese oxide MnO_2. X-ray phase analysis of the samples showed that all solid solutions crystallize in the perovskite structure without impurity phases. Figure 2 shows diffraction peaks $(200)_C$ of solid solutions superstoichiometrically and stoichiometrically modified by MnO_2. It can be seen that the insertion of 1 mass.% MnO_2 into the initial solid solution increases the intensity of peak 020 corresponding to the monoclinic distortion of the perovskite cell, which suggests the appearance of a second phase coherently coupled with the initial matrix along the plane (020). X-ray analysis showed that the symmetry of the second phase is tetragonal (T). The content of the T-phase increases with an increase of the concentration of MnO_2. The symbatic change of the concentration of MnO_2 and the T-phase indicates that Mn^{4+} is incorporated into the solid solution structure.

No clear correlation is observed between the concentration of the modifier and the solid solution phase composition in case of the stoichiometric modification by MnO_2 (Figure 2, *b*). The intensity of peak 020 increases in samples with $x = 0.0125$, 0.0375 compared to the initial solid solution due to the occurrence of the T-phase. But the peak 020 splits into two peaks at $x = 0.025$, and its intensity decreases again (the second peak is shown by an arrow in Figure 2, *b*); a slight splitting is also visible at peak 200.

From this it can be concluded that there is another low-symmetry phase. The traces of this phase are still visible at $x = 0.0375$. We reflected the phase composition of solid solution in the range of $0.0125 < x \leq 0.0375$ as a mixture of R(M)-, T- and pseudocubic (PSC) phases due to the uncertainty of the diffraction pattern.

Therefore, it is possible to conclude that solid solution crystal lattice contains Mn^{4+} in both modification schemes, but its position in the structure is different.

Figure 3 shows the dependences of parameters $a = c$, b, angle β and volume V of the monoclinic cell of the main R(M) phase of the modified solid solution on x. Figure 3, *a* shows that the largest variation of all parameters in case of superstoichiometric modification is observed in the range of $0 < x \leq 1$ mass.%. The parameters a and V monotonously decrease with the further growth of x, but V does not reach the initial value. Notwithstanding that the cell parameters vary within the measurement error (with the exception of b), the solid solution phase composition gradually changing with the growth of x suggests that the behavior of the structural parameters is reliable.

Since Mn^{4+} has the smallest ionic radius among all B-cations (see Table 2), the initial increase of V can only be attributed to the formation of a interstitial solid solution, and its subsequent decrease can be attributed to the formation of a solid solution of $Mn^{4+} \to (Nb^{5+}, Ta^{5+})$ substitution. On the other hand, the changes of volume are so small that, most likely, these two processes are concurrent which results in the appearance of local areas of interstitial solid solutions and substitutional solids solutions of $Mn^{4+} \to$ B-cation, and the number of the former decreases with the growth of x, and the number of latter increases. In fact, we have a pattern of a morphotropic phase transition R(M) → T, and it is possible to expect the appearance of abnormal electrical properties here.

Figure 3, b shows the dependences of parameters of the perovskite cell of the main monoclinic phase on x in case of stoichiometric modification of the initial composition by manganese oxide. It can be seen that V of the cell decrease in the range of $0.0 < x \leq 0.025$ in accordance with the modification formula, which assumes the formation of a substitutional solid solution. The sharp increase of V with $x = 0.0375$ is probably attributable to the formation of anionic vacancies when an ion with a large charge is replaced by an ion with a smaller charge, which results in the swelling of the crystal lattice. The formation of insertion solid solutions is also possible or substitution of cations in B positions with manganese ions of lower valence ($R^6_{Mn^{3+}} = 0.70$ Å, $R^6_{Mn^{2+}} = 0.91$ Å).

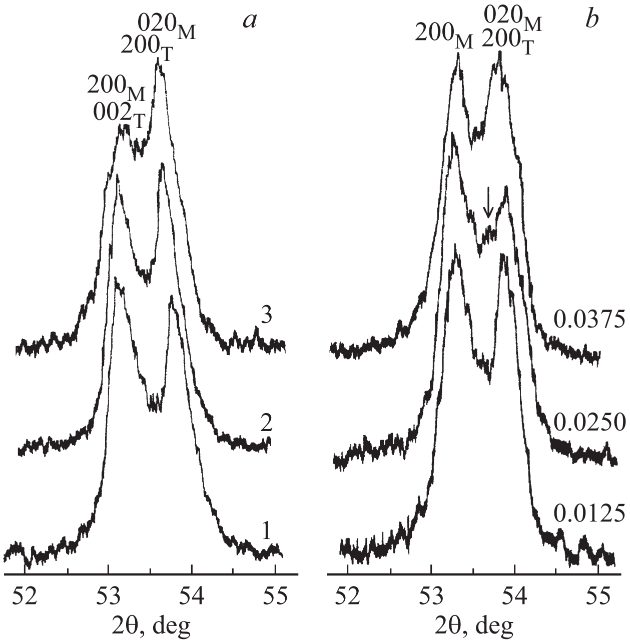

Figure 2. Diffraction peaks $(200)_C$ of the initial solid solution, a) superstoichiometrically (numbers in the right side — mass.%) and b) stoichiometrically (numbers in the right side — x) modified by MnO_2.

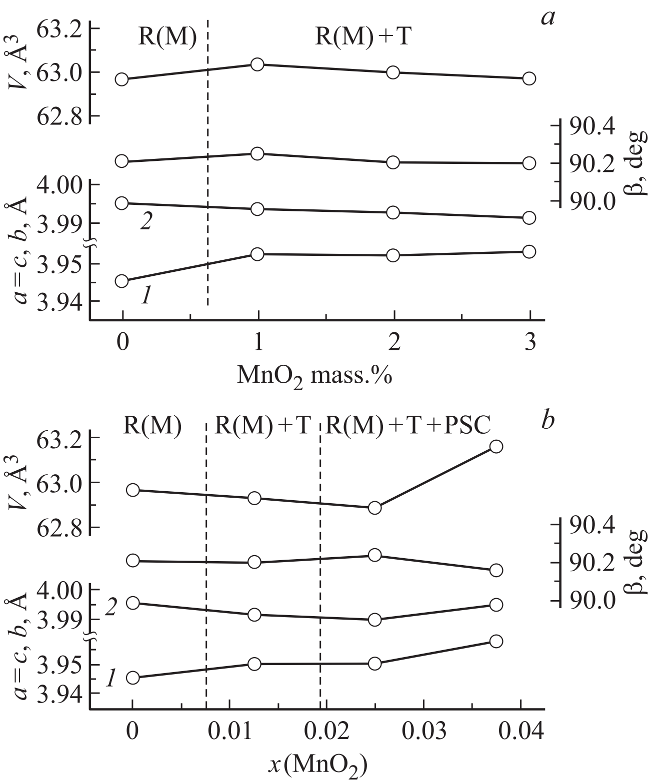

Figure 3. Dependences of the parameters of the perovskite monoclinic cell of the initial solid solution, a) superstoichiometrically and b) stoichiometrically modified by MnO_2, on the modifier concentration: curve 1 — b, 2 — $a = c$.

Figure 4 shows the dependences of the densities of solid solution ceramics with a different scheme of modification by manganese oxide. It can be seen that the modification significantly increases the density of the initial solid solution in both cases. However, the relative density of ceramics increased by 8% in case of superstoichiometric modification and by 5% in case of stoichiometric modification. High densities do not change in case of superstoichiometric modification and decrease in case of stoichiometric modification with an increase of the modifier concentration. That is, in the first case, solid solutions are more resistant to small fluctuations of the modifier concentration, which is essential in case of usage of alkaline elements. A very precise stoichiometry is required to achieve maximum ceramic density in the second case.

Let us consider the complex modification of solid solution of $0.98(Na_{0.54}K_{0.46})(Nb_{0.9}Ta_{0.1})O_3{-}0.02LiSbO_3$ -2 mass.% $NiO{+}MnO_2$.

Addition of 2 mass.% NiO in the original solid solution makes it even more heterogeneous than in case of modification by MnO_2. This is evidenced by the diffraction peaks $(200)_C$ shown in Figure 5. A mixture of two phases is observed in superstoichiometrically modified solid solutions (Figure 5, a) with all concentrations of MnO_2:

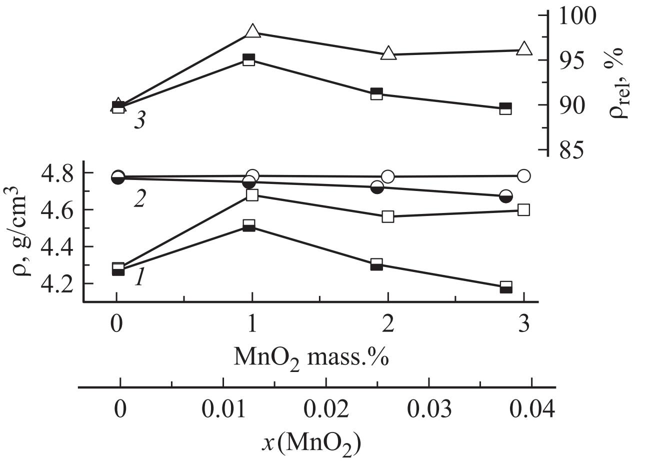

Figure 4. Dependences of experimental (curves *1*), X-ray (*2*) and relative (*3*) densities of initial solid solution ceramics on the concentration (x) of MnO_2. The densities of superstoichiometrically and stoichiometrically modified samples are indicated by empty and filled symbols, respectively.

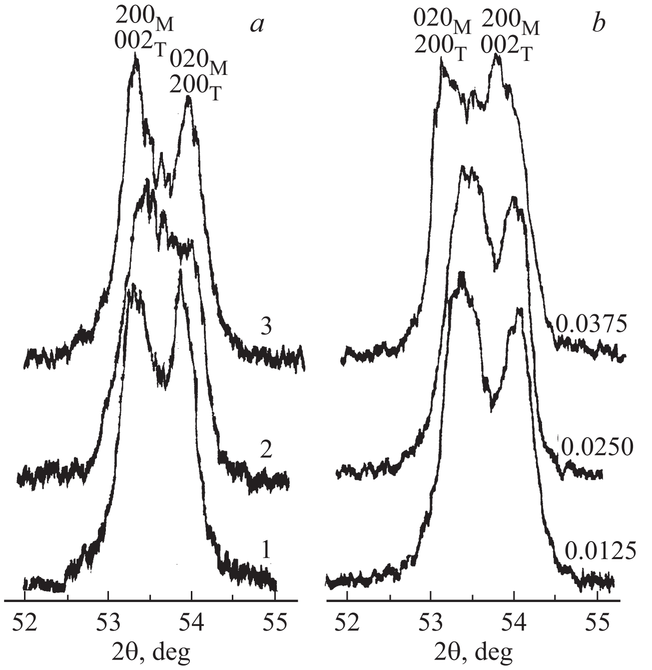

Figure 5. Diffraction peaks $(200)_C$ of the initial solid solution with NiO oxide, *a*) superstoichiometrically (numbers in the right side — mass.%) and *b*) stoichiometrically (numbers in the right side — x) modified by MnO_2.

R(M) and T, with the largest amount of T-phase present in solid solution with 1 mass.% MnO_2; the solid solution is very heterogeneous with 2 mass.%. The complexity of the phase composition gradually increases from the R(M)-phase in the initial solid solution to a mixture of two phases R(M)+T with $x = 0.0125$ in stoichiometrically modified solid solutions (Figure 5, *b*) with the increase of the MnO_2 concentration, and then another phase, PSC, is added to them, the symmetry of which cannot be definitively determined because of the strong smearing and superposition of X-ray peaks. The content of T-phases and PSC phases increases with an increase of MnO_2 concentration.

Figure 6 shows the dependences of the parameters of the perovskite monoclinic cell of the main R(M) phase on MnO_2 concentration. The change of structural characteristics has a same nature in case of both modification schemes, but the V of cells decreases by $\Delta V = -0.28\,\text{Å}^3$ in superstoichiometrically modified solid solutions (Figure 6, *a*) with 1 mass.% MnO_2, and the cell volume V decreases by $\Delta V = -0.32\,\text{Å}^3$ in stoichiometrically modified solid solutions (Figure 6, *b*) with $x = 0.0125$; V monotonously increases with a further increase of MnO_2 concentration.

This means that $Mn^{4+} \rightarrow$ B-cation substitution takes place in both cases with a minimum amount of MnO_2. The increase of V can be caused either by the dissolution of Mn^{4+} ions in the crystal lattice with the formation of interstitial solid solutions, or the formation of substitutional solid solutions with Mn^{3+} or Mn^{2+} ions in the B-positions. Both of these processes can take place. It is difficult to predict the final result taking into account the probable substitutions of Ni^{2+} ions with Mn^{4+} ions.

Figure 7 shows the dependences of ceramic densities on the concentration of manganese oxide. It can be seen that the density of superstoichiometrically modified ceramics

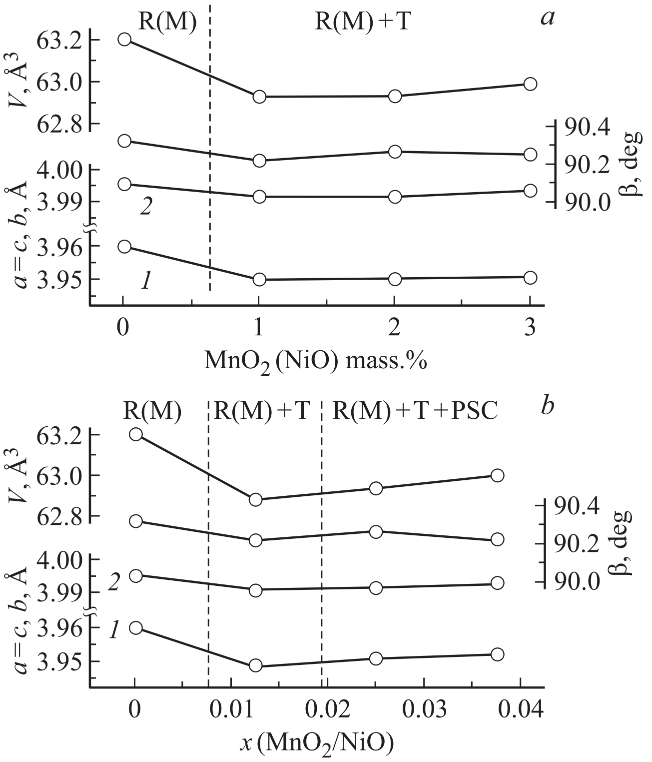

Figure 6. Dependences of the parameters of the perovskite monoclinic cell of the initial solid solution with 2 mass.% NiO, *a*) superstoichiometrically and *b*) stoichiometrically modified by MnO_2 on x: curves *1* — b, *2* — $a = c$.

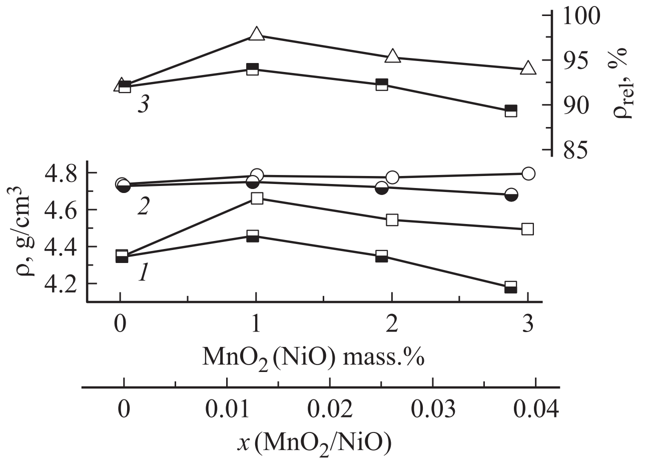

Figure 7. Dependences of experimental (curves *1*), X-ray (*2*) and relative (*3*) densities of ceramics of the initial solid solution with 2 mass.% NiO on the concentration of the inserted MnO_2 in case of superstoichiometric (empty symbols) and stoichiometric (filled symbols) modification.

is higher in case of the complex modification, than the density of stoichiometrically modified ceramics, the density reaches maximum values with the lowest concentration of MnO_2. The relative density of the superstoichiometrically modified solid solution is 3.5% higher than the density of stoichiometrically modified ceramics, and it is 5.6% higher than the density of the initial solid solution.

The same pattern is observed in case of monomodification by MnO_2, but in that case the densities are not so sensitive to variations of the composition of solid solution. This, as well as a less complex phase composition and greater homogeneity of solid solution in case of monomodification, make this scheme more preferable.

Let us consider the superstoichiometric modification of CuO.

Superstoichiometric modification of the initial solid solution by copper oxide, as well as by MnO_2, results in the appearance of a T-phase, which has the maximum content with 2 mass.% CuO and minimum content with 3 mass.% (Figure 8).

Figure 9 shows the dependences of the parameters of the monoclinic cell of the main R(M) phase and the densities of solid solution ceramics on the concentration of CuO. Figure 9, *a* shows that the change of the linear parameters and volume of the perovskite cell with an increase of the concentration of CuO is non-monotonic. This suggests a complex and ambiguous mechanism of distribution of Cu^{2+} ions in the structure. The decrease of *V* with 1 mass.% can be caused by $Cu^{2+} \rightarrow Na(K)$ substitution, and it can have microscopic quantities due to the large difference of EN (see Table. 2); the increase of *V* with 2 mass.% may be associated with the formation of solid solutions of $Cu^{2+} \rightarrow$ B-cation substitution whose radii are significantly smaller than the radius of Cu^{2+} (see Table 2). The decrease of *V* at 3 mass.% CuO may be caused by the decomposition

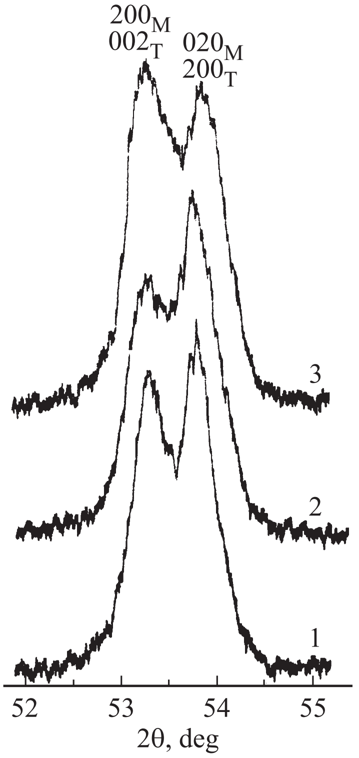

Figure 8. Diffraction peaks (200)C of initial solid solution, superstoichiometrically modified by CuO (numbers in the right side— mass.%).

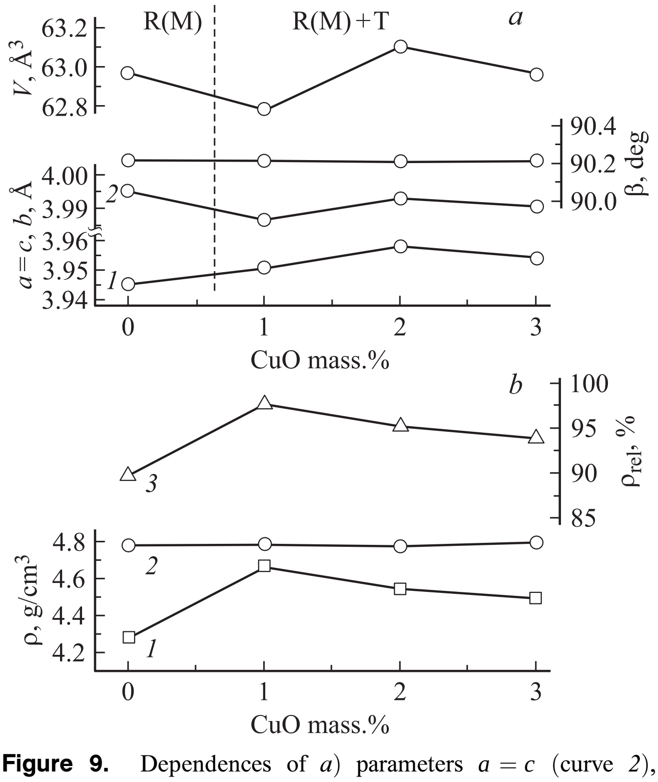

Figure 9. Dependences of *a*) parameters $a = c$ (curve *2*), *b* (*1*), *β*, *V* of perovskite monoclinic cell and *b*) experimental (curve *1*), X-ray (*2*) and relative (*3*) densities of ceramics of initial solid solution, superstoichiometrically modified by CuO on the concentration of CuO.

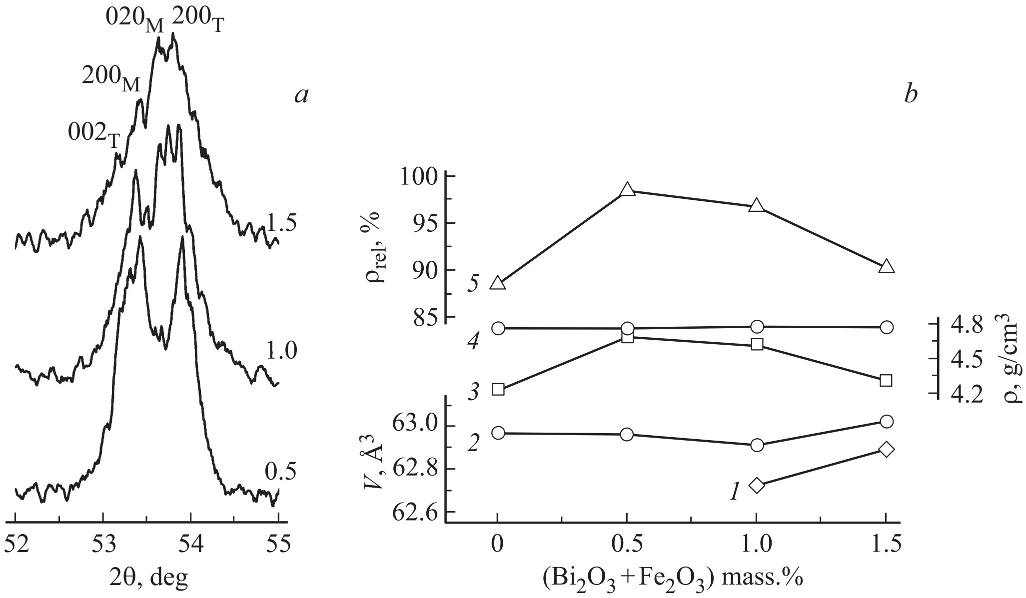

Figure 10. *a*) Diffraction peaks $(200)_C$ (numbers in the right side — mass.%), *b*) dependences of the cell volume and ceramic densities of the initial solid solution, superstoichiometrically modified by $Bi_2O_3+Fe_2O_3$ oxides on the modifier concentration: curve *1* — V_M, *2* — V_T, *3* — ρ_{exp}, *4* — $\rho_{X\text{-}ray}$, *5* — ρ_{rel}.

of supersaturated solid solution which results in the decrease of the amount of T-phase (Figure 8). Figure 9, *b* shows that the modification of the original solid solution by 1 mass.% CuO increased the relative density of ceramics by 7.9% compared to the density of nonmodified ceramics. A further increase of the modifier concentration resulted in a decrease of the density.

Let us consider the superstoichiometric modification by $Bi_2O_3+Fe_2O_3$ oxides.

As in the samples discussed above, the superstoichiometric introduction of 0.5 mass.% $Bi_2O_3+Fe_2O_3$ into the initial solid solution leads to the appearance of the second phase — tetragonal, the content of which increases with the increase of the concentration of $Bi_2O_3+Fe_2O_3$ (Figure 10, *a*). Figure 10, *b* shows the dependences of the volume V of perovskite cell and ceramic densities on the concentration of $Bi_2O_3+Fe_2O_3$. It can be seen that the cell volume decreased by $\Delta V = -0.06\,\text{Å}^3$ in the range of 0.0–1.0 mass.% $Bi_2O_3+Fe_2O_3$, and it increased by $\Delta V = 0.11\,\text{Å}^3$ at 1.5 mass.% and exceeds the cell volume of the initial solid solution. The absence of extraneous lines on the X-ray pattern, changes of the phase composition and volume of the cell of the initial solid solution indicate that modifier ions are incorporated into the crystal lattice of the initial solid solution in case of superstoichiometric modification. Given that the ionic radii of Nb^{5+}, Ta^{5+} and Fe^{3+} are practically the same (see Table 2), it can be assumed that the decrease of the cell volume is associated with the formation of solid solution of $Bi^{3+} \rightarrow K^{1+}$ substitution.

However, the difference of electronegativities of Bi and K (Table 2) is almost three times higher than the permissible value of 0.4 [26], therefore, $Bi^{3+} \rightarrow K^{1+}$ substitution can take place only at a microscopic scale, which may explain the small decrease of the cell volume. The increase of the volume can be caused by several reasons: $Bi^{3+} \rightarrow Na^{1+}$ substitution, insertion of Fe^{3+} and/or O^{2-} ions formed during the substitution of a cation with a lower charge (K^{1+}) by a high-charge cation (Bi^{3+}) into the crystal lattice. The density of ceramics, as in previous cases, is maximum in the composition with the lowest amount of modifier, and its relative density exceeds the density of the initial solid solution by 10%.

Thus,common patterns of modification of solid solution of $0.98(Na_{0.54}K_{0.46})(Nb_{0.9}Ta_{0.1})O_3-0.02LiSbO_3$ composition were established:

– modification, both stoichiometric and superstoichiometric, results in the appearance of a second — tetragonal phase inside the rhombic R(M) phase, that is, it takes solid solution to the morphotropic phase transition region;

– both modification schemes increase the density of the modified ceramics in comparison with the density of the original solid solution, and solid solutions with a minimum amount of modifier have the maximum density;

– the increase of relative density by 8–10% compared to the initial solid solution was associated with superstoichiometric modification;

– the resistance of the structure to small variations of composition was determined in superstoichiometrically modified solid solutions.

Based on the combination of structural characteristics, ceramic density and its resistance to small variations of composition, it is possible to conclude that MnO_2 and $Bi_2O_3+Fe_2O_3$ are the most promising modifiers in case of superstoichiometric modification.

Table 3. Electrophysical characteristics of the best solid solutions studied

Modifiers	Parameters					
	T_C, °C	$\varepsilon_{33}^T/\varepsilon_0$	$\lvert d_{31}\rvert$, pC/N	K_p	Q_M	V_1^E, km/s
MnO_2	340	400	35	0.25	500	4.8
$Bi_2O_3+Fe_2O_3$	420	500	55	0.45	170	4.6

These particular solid solutions (with one mass.% of modifiers) are characterized by the best piezo properties with low values of $\varepsilon_{33}^T/\varepsilon_0$ (Table 3), which makes it possible to recommend them for applications in microwave technology.

4. Conclusion

Solid solutions were studied on the basis of a multi-element system of $0.98(Na_{0.54}K_{0.46})(Nb_{0.9}Ta_{0.1})O_3-0.02LiSbO_3$ composition, modified by simple (MnO_2, CuO) and combined $(MnO_2+NiO,\ Bi_2O_3+Fe_2O_3)$ oxides superstoichiometrically inserted in quantities of $1-3$ mass.% and stoichiometrically inserted in quantities of $x = 0.0125-0.0375$. The samples were obtained by two-stage solid-phase synthesis followed by sintering using conventional ceramic processing.

It was found by X-ray studies that the initial solid solution has rhombic symmetry with a monoclinic perovskite cell R(M). Modification of solid solutions by these modifiers, both stoichiometric and superstoichiometric, leads to the appearance of a second — tetragonal phase inside the R(M) phase, that is, it takes the solid solution to the morphotropic phase transition region. It is shown that both modification schemes increase the density of the modified ceramics in comparison with the density of the original solid solution, and solid solutions with a minimum amount of modifier have the maximum density. The resistance of the structure to small variations of composition was determined in superstoichiometrically modified solid solutions. A conclusion was made that MnO_2 and $Bi_2O_3+Fe_2O_3$ are the most promising modifiers of the studied solutions in case of superstoichiometric modification. Compositions with optimal piezoelectric parameters for microwave technology applications were selected. The obtained results shall be preferably used for development of similar materials and devices based on these materials.

Funding

This study was supported financially by the Ministry of Science and Higher Education of the Russian Federation (state research assignment. Project No. FENW-2023-0010/GZ0110/23-11-IF), topic: „Multicomponent intelligent structures: phase-shifting crossing effects and strategies for accelerated ecosystem designing for technologies of digital designing of devices for monitoring physical media parameters“. Equipment was provided by the Center for the Collective Use of Scientific Equipment of the Research Institute of Physics, Southern Federal University, „Electromagnetic, Electromechanical and Thermal Properties of Solid Bodies“.

Conflict of interest

The authors declare that they have no conflict of interest.

References

[1] B. Jaffe, W.R. Cook, H. Jaffe. Piezoelectric Ceramics. Academic Press, N.Y. (1971). 317 p.

[2] A.J. Danziger, O.N. Razumovskaya, L.A. Reznichenko, V.P. Sakhnenko, A.N. Klevtsov, S.I. Dudkina, L.A. Shilkina, N.V. Dergunova, A.N. Rybyanets. Mnogokomponentnye sistemy segnetoelektricheskih slozhnyh oksidov: fizika, kristallohimiya, tekhnologiya. Aspekty dizajna p'ezoelektricheskih materialov. MP „Kniga“, Rostov-on-Don. (2001−2002). T. 1, 2. 800 s. (in Russian).

[3] J. Yoo, K. Lee, K. Chung, S. Lee, K. Kim, J. Hong, S. Ryu, C. Lhee. Jpn. J. Appl. Phys. **45**, *9S*, 7444 (2006).

[4] B.-Q. Ming, J.-F. Wang, P. Qi, G.-Z. Zang. J. Appl. Phys. **101**, *5*, 054103 (2007).

[5] Z. Yang, Y. Chang, L. Wei. Appl. Phys. Lett. **90**, *4*, 042911 (2007).

[6] F. Rubio-Marcos, P. Ochoa, J.F. Fernandez. J. Eur. Cer. Soc. **27**, *13−15*, 4125 (2007).

[7] Y. Guo, K.-I. Kakimoto, H. Ohsato. Mater. Lett. **59**, *2−3*, 241 (2005).

[8] S. Zhang, R. Xia, T.R. Shrout, G. Zang, J. Wang. J. Appl. Phys. **100**, *10*, 104108 (2006).

[9] J.G. Wu, Y.Y. Wang, D.Q. Xiao, J.U. Zhu, P. Yu, L. Wu, W.J. Wu. Jpn. J. Appl. Phys., **46**, *11R*, 7375 (2007).

[10] T.R. Shrout, S.J. Zhang. J. Electroceram. **19**, *1*, 111 (2007).

[11] W. Yang, D. Jin, T. Wang, J. Cheng. Physica B **405**, *7*, 1918 (2010).

[12] H. Du, F. Tang, F. Luo, D. Zhu, S. Qu, Z. Pei, W. Zhou. Mater. Res. Bull. **42**, *9*, 1594 (2007).

[13] T. Lee, K.W. Kwok, H.L. Li, H.L.W. Chan. Sens. Actuators A **150**, *2*, 267 (2009).

[14] J. Fu., R. Zuo, X. Fang, K. Liu. Mater. Res. Bull. **44**, *5*, 1188 (2009).

[15] H.L.W. Chan, S.H. Choy, C.P. Chong, H.L. Li, P.C.K. Liu. Ceram. Int. **34**, *4*, 773 (2008).

[16] R. Gaur, K.C. Singh, R. Laishram. Ceram. Int. **41**, *1 Part B*, 1413 (2015).

[17] G. Ray, N. Sinha, S. Bhandari, B. Kumar. Scripta Materialia **99**, 77 (2015).

[18] X. Huo, R. Zhang, L. Zheng, S. Zhang, R. Wang, J. Wang, S. Sang, B. Yang, W. Cao. J. Am. Ceram. Soc. **98**, *6*, 1829 (2015).

[19] I.A. Verbenko, O.N. Razumovskaya, L.A. Shilkina, L.A. Reznichenko. V sb. materialov X Mezhdunarodnogo mezhdisciplinarnogo simpoziuma „Poryadok, besporyadok i svojstva oksidov" („ODPO-2007". Rostov-on-Don. (2007). S. 140). (in Russian).

[20] I.A. Verbenko, O.N. Razumovskaya, L.A. Shilkina, L.A. Reznichenko, K.P. Andryushin. Inorg. Mater. **45**, *6*, 702 (2009).

[21] I.A. Verbenko, O.N. Razumovskaya, L.A. Shilkina, L.A. Reznichenko, K.P. Andryushin, V.V. Kilessa. Inorg. Mater. **45**, *7*, 814 (2009).

[22] A.G. Abubakarov, L.A. Shilkina, I.N. Andryushina, K.P. Andryushin, I.A. Verbenko, L.A. Reznichenko, A.V. Nagaenko, S.A. Zeilinger, H.A. Sadykov. Konstrukcii iz kompozicionnyh materialov *3 (147)*, 53 (2017). (in Russian).

[23] A.G. Abubakarov, H.A. Sadykov, L.A. Shilkina, I.A. Verbenko, A.G. Silcheva, L.A. Reznichenko. Vestnik Luganskogo nacional'nogo universiteta im. Vl. Dalya. **2**, *40*, 15 (2017). (in Russian).

[24] L.I. Mirkin. Spravochnik po rentgenostructurnomu analizu polikristallov. Fizmatgiz, M. (1961). 863 s. (in Russian).

[25] IEEE Standard on Piezoelectricity ANSI/IEEE Std 176–1987, N.Y. (1988).

[26] V.S. Urusov. Teoriya izomorfnoj smesimosti. Nauka, M. (1977). 251 s. (in Russian).

[27] G.B. Bokiy. Vvedenie v kristallokhimiyu. Izd-vo MGU, M. (1954). S. 120. (in Russian).

[28] L. Pauling. General Chemistry. W.H. Freeman, San-Francisco (1970). 851 p.

Translated by A.Akhtyamov